

Liquid Metal Droplet Tunable RF MEMS Inductor

Issam El Gmati^{1,2}, Ridha Ghayoula³

¹College of Engeneering Al Qunfudha Umm al Qura University, KSA

²Higher school of sciences and technology of Hammam Sousse, Tunisia

³Department of Electrical and Computer Engineering, Laval University, Quebec City, Canada

Abstract: A new variable inductor has been simulated, manufactured and tested. The idea is based on changing the morphology of a Galinstain droplet by electrostatic actuation. A drop of 200 μm diameter is used and the applied voltage is limited to 100 V. We demonstrate a tunable inductor that simultaneously achieves wide tuning range of 400 % with high inductance from 1.8 nH to 9.1 nH with a measured quality factor of 26 at 2 GHz and the self-resonance frequency is 4 GHz. Their results were compared. The conclusion showed that simulation results matched well with measurement. The Comparison between our work and other published works show excellent performance.

Keywords: Tunable inductor, radiofrequency, MEMS, droplet, Galinstain

Nastavljiva mikrofluidna RF MEMS tuljava

Izveček: Simuliran, izdelan in preizkušen je bil nova spremenljiva tuljava. Zamisel temelji na spreminjanju morfologije kapljice Galinstain z elektrostatičnim vzbujanjem. Uporabljena je kapljica s premerom 200 μm , napetost pa je omejena na 100 V. Prikazali smo nastavljivo tuljavo, ki hkrati dosega široko območje nastavitve 400 % z visoko induktivnostjo od 1,8 nH do 9,1 nH z izmerjenim faktorjem kakovosti 26 pri 2 GHz, samorezonančna frekvenca pa je 4 GHz. Njihovi rezultati so bili primerjani. Zaključek je pokazal, da se rezultati simulacije dobro ujemajo z meritvami. Primerjava med našim delom in drugimi objavljenimi deli je pokazala odlično učinkovitost.

Ključne besede: nastavljiva tuljava, radio frekvenca, MEMS, kaplica, Galinstain

* Corresponding Author's e-mail: iagmati@uqu.edu.sa

1 Introduction

Passive RF MEMS (Radiofrequency Micro-Electro-Mechanical Systems) components play a primary role in modern transceiver and receiver architectures. They provide significant gains in terms of miniaturization, motivating performance in the gigahertz band as well as low power consumption. Many MEMS components have been developed for radio frequency application; in particular inductors. Micro inductors are used in, for example, RF MEMS [1–8], micro-actuators [9–11], bio-sensors [12], micro-actuators [13], power MEMS [14], energy harvesters [15], transformers and electromagnetic motors [16]. Most inductors have fixed inductance value. The new generations of communications systems, on the other hand, aim to use very wide frequency bands to simplify these systems, reduce the number of transmission / reception channels, and consequently reduce their costs. To achieve these

goals, it is important to replace fixed components with variable components. [17]. Variable inductors have the same performance as fixed inductors; to vary inductance. We can play on several geometric or technological parameters as well as on the variation techniques [18]. In the work [19] and in order to vary the inductance having discrete values, the researchers used micro-relays. Other techniques have been invented by modifying the magnetic flux [20–21], or by playing on mutual inductance [22–23]. Other works have proposed the micro-fluidic action by using liquids [24–26]. The common objective of all this work is to achieve a good variation of the inductance, a good quality factor as well as a high resonant frequency in the gigahertz band allowing the integration of these components in the application devices. Until today, none of the published structures have corresponded to our objectives, namely a high variation ratio, a good quality factor, a

How to cite:

I. El Gmati et al., "Liquid Metal Droplet Tunable RF MEMS Inductor", Inf. Midem-J. Microelectron. Electron. Compon. Mater., Vol. 53, No. 1(2023), pp. 31–37

variable inductance working in the gigahertz bands. In order to achieve our goals, we were able to design a new method to vary the inductance. The idea is to slide a droplet of Galinstain horizontally above the inductor and control it by electrostatic actuation. The structure is manufactured and tested. Good performances have been shown.

2 Design of inductance

Figure 1 shows the model of the designed inductance and the principle used to vary the inductance. The structure consists of a planar spiral inductor and a liquid metal such as Galinstain. The metal drop is placed above the spiral inductor.

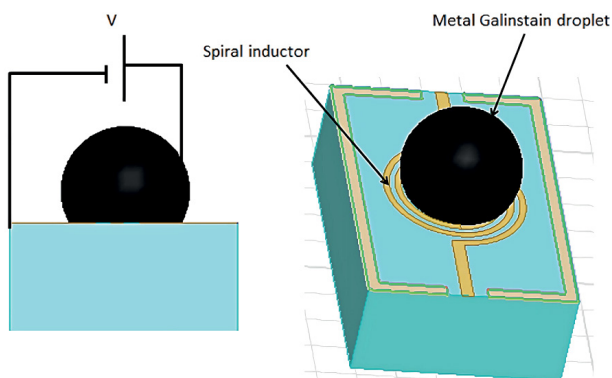


Figure 1: Model of the designed inductance and principle used to vary the inductance.

The planar inductor fabricated on a glass substrate; designed in double circular form with 3 turns with a coil 20 μm wide, spaced 20 μm . The length of the internal diameter is 600 μm so the external one is 1200 μm . The basic idea is to place a drop above the metal coils and thus modify the geometric parameters of the inductance by short-circuiting a portion of the coil. This allows a reduction in the current path and consequently a change in the inductance value. Figure 2 shows the steps followed in a clean room to fabricate the inductor. The gold coils were deposited on a glass substrate. This manufacturing process requires 3 masks.

A Ti/Au (500 \AA /500 \AA) seed layer was regularly popped on highest side of a 500 μm thick glass substrate. The Ti layer was placed to improve the bond, and a positive photoresist (AZ 4562) was next spotted in order to form the electroplating mould (thickness $\approx 5.5 \mu\text{m}$). A 2 μm thick gold were electroplated into the resist mould. The photoresist mould was then removed and the seed layer was chemically etched. Finally, a droplet of 200 μm is used and the applied bias voltage is limited to 100 V. Figure 3 shows a top view of the circular shaped inductor made of gold on a glass substrate.

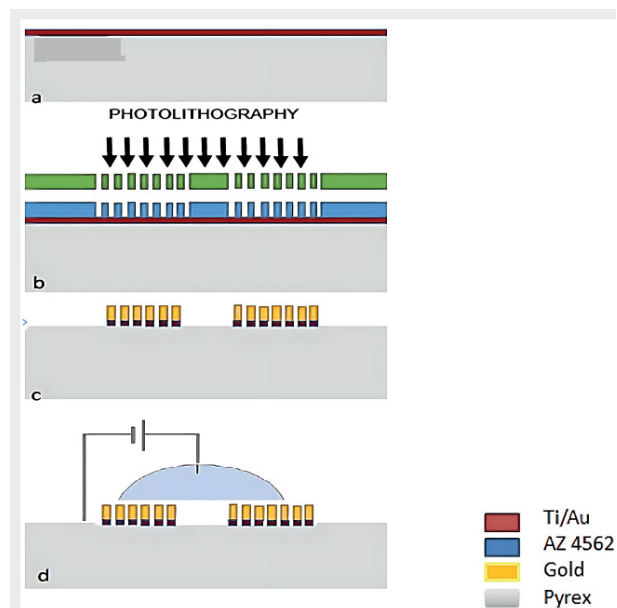


Figure 2: Schematic cross section of the fabricated inductor.

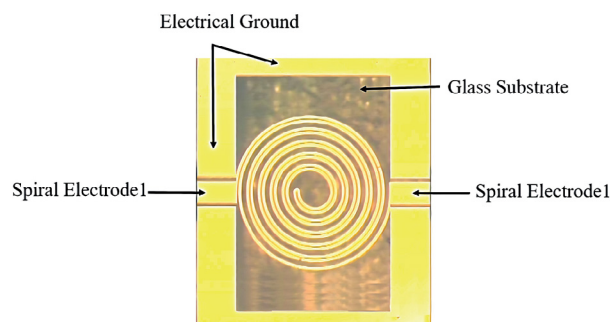


Figure 3: Photography of one inductor under fabrication.

Table 1 shows physical properties of materials used in fabrication process.

Table 1: Physical properties of materials used in fabrication process.

Materials	Relative Permittivity	Dielectric Loss	Relative Permeability	Bulk Conductivity (S/m)
Glass	5.5	0.0037	1	0
Gold	1	0	0.99996	41E6

3 Results and discussion

This section may be divided by subheadings. It should provide a concise and precise description of the experi-

mental results, their interpretation, as well as the experimental conclusions that can be drawn. The measurements shown in figure 4 were carried out under spikes with a vector network analyzer (VNA 'Vector Network Analyzer') HP 8510 which has a frequency range of 50 MHz-13 GHz using GSG 'Ground Signal Ground' micro-probe RF tips. The inductance L and the quality factor Q were calculated by using the following equations [27]

$$L = \frac{1}{2\pi f} \operatorname{Im} \left(\frac{1}{Y_{11}} \right) \quad (1)$$

$$Q = \frac{\operatorname{Im} \left(\frac{1}{Y_{11}} \right)}{\operatorname{Re} \left(\frac{1}{Y_{11}} \right)} \quad (2)$$

Y^{ind} , Y^{meas} and Y^{open} are the two-port admittance matrix the admittance matrices of the measured inductor and the open pattern, respectively.

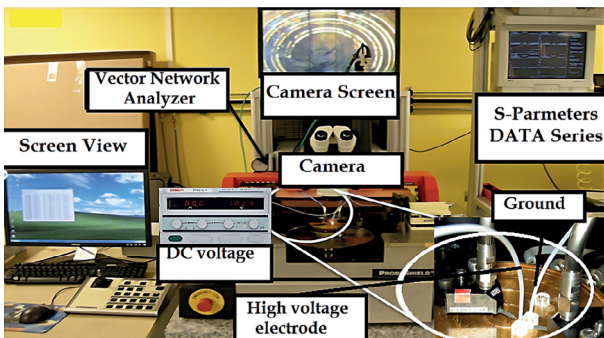


Figure 4: Test bench for S-parameters characterization.

During the measurements droplets of Galinstain [28] with conductivity of the order than $3.46 \cdot 10^6 \text{ S/m}$ at 20°C were used. The inductance varies by touching the liquid metal droplet upon the spiral inductor shown in figure 5. The Galinstain droplet is flattening out as applying a voltage. Measurements were taken for 6 voltage levels applied to the liquid metal droplet for a frequency span of 100 MHz to 10 GHz.

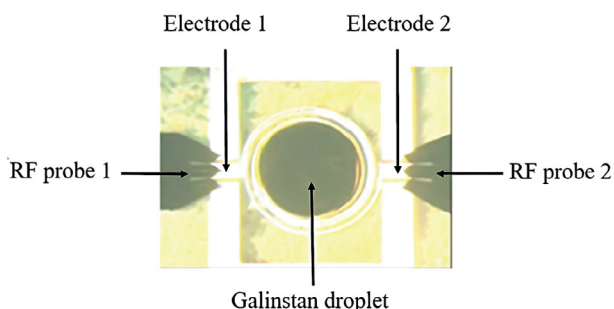


Figure 5: Galinstain droplet placed above the spiral inductor for different applied voltage.

As shown in figure 6 (a) the inductor has a peak of 25 at 2 GHz, and the self-resonance frequency is 4 GHz. The quality factor decreases from $Q_{\text{max}} = 26$ when the applied voltage is 100 V to $Q_{\text{min}} = 12$ when it is equal to 0 V. As demonstrated in figure 6(b), the measured inductance at high frequency increases continuously between $L_{\text{min}} = 1.8 \text{ nH}$ and $L_{\text{max}} = 9.1 \text{ nH}$ at 2 GHz by applying voltage. A 400 % tuning range is achieved at 2 GHz.

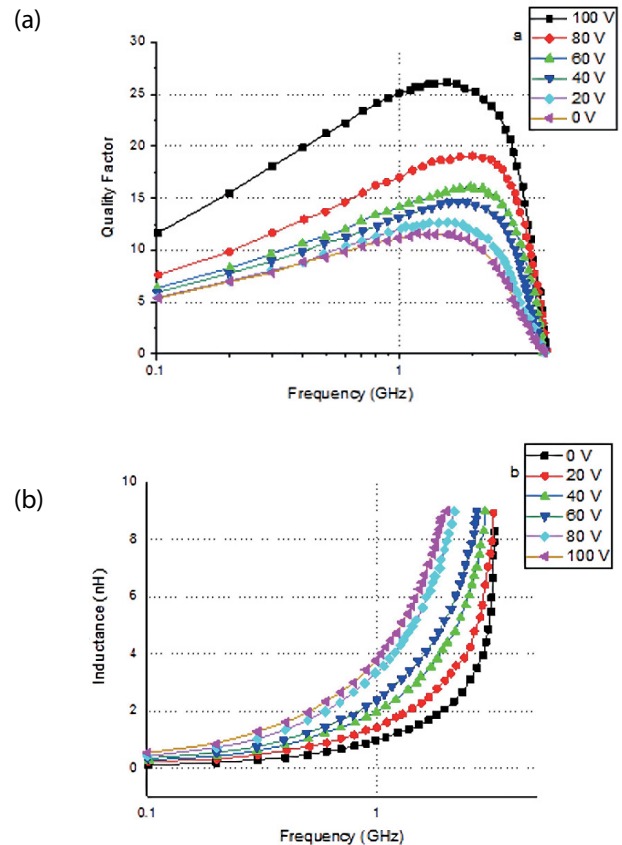


Figure 6: Measured results a Quality factor by frequency (a) and inductance (b) of a fabricated tunable RF MEMS inductor by applied voltage.

HFSS (3D Electromagnetic Field Simulator for RF and Wireless Design) software was used to simulate an inductor 3D model structure. Figures 6 show the variations of the measured results as a function of the voltage at a frequency of 2 GHz.

When the Galinstain droplet is present on the metal coils, it short-circuits a portion of the coil allowing a reduction in the number of coils of the inductance and subsequently a decrease in the value of the inductance. On the other hand, this reduction in the number of turns allows an increase in the quality factor shown in figure 7(a). The inductance L varies proportionally as a function of the number of coils N . The variation in the quality factor is inversely proportional to N .

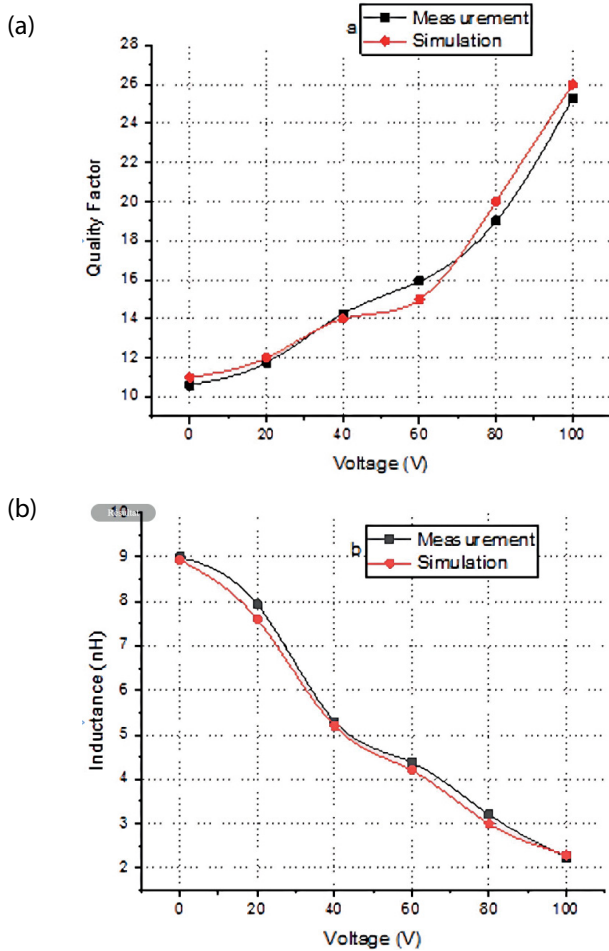


Figure 7: Comparison between simulated and measured inductance (a) and Quality Factor (b) of the tunable inductance at 2 GHz by applied voltage.

Variations in inductance shown in figure 7 (b) values have been visualized for different Galinstain contact pins on metal coils. You can notice a slight difference of around 5% between the measurement results and the simulation results. This can be attributed to other factors due to the existence of an external potential. The position of the liquid droplet above the metal coil may cause this slight difference. In fact, the drop can either be in direct contact with the gold turns, or it can form a capacitive contact through a thin layer.

In the presence of the Galinstain droplet, the magnetic flux of the inductance infiltrates the Galinstain droplet causing the creation of an eddy current inducing a counteractive magnetic field according to Lenz's law causing magnetic loss. When the droplet is moved away from the metal spires, the inductance exhibits very low loss.

A comparison of the measurement results of this variable inductance with others published and presented in Table 2.

Table 2: Performance comparison published works and our work.

Operating Frequency GHz	Inductance	Quality factor	Tunability%	Ref
6	1.1	46	47.5	[29]
1	8.86	25.5	27.7	[30]
2.5	3.3	>20	230	[31]
2	0.93	0.96	10	[32]
1.5	1.2	2.87	191	[33]
4	0.3	8	60	[34]
5	1.2-2.3	38.2	90	[35]
4	2.8	18	380	[36]
2	1.8-9.1	26	400	This work

We can notice that our inductor showed good performance in terms of variation, quality factor as well as reasoning frequency by comparing it with other works. The inductance produced is an ambitious solution in terms of small size in micrometers, energy consumption, low cost meeting the objectives set at the beginning such as a good inductance variation of the order of Nano-henry, a good quality factor in the Gigahertz frequency band and a resonance frequency of the order of Giga-hertz. The works cited in Table 1; not been able to group all these constraints together. To implement this inductor in real applications, you would need a wrapper or something to keep the liquid metal from moving around.

The inductance is modelled by L_s and the finite conductivity of the metal is represented with the series resistance R_s . The capacitive coupling of the windings between the input and output is modelled by C_s shown in Figure 8.

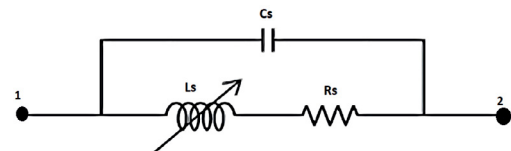


Figure 8: Electric Equivalent model for tunable inductor.

The compact model was fitted to the measured S-parameters. The fitted model parameters for different applied voltage are listed in Table 3.

Table 3: Fitted compact model parameters from Measured.

Frequency GHz	Applied voltage	Ls (nH)	Rs (Ω)	Cs (fF)
2	0	9.1	10	0.83
2	20	8	13	0.85
2	40	5.25	15	0.87
2	60	4.3	17	0.91
2	80	3.1	20.4	0.98
2	100	1.8	24	1.01

The fitted L_s correspond to the measured results in Figure 6 (b). The R_s does fluctuate with injected fluid, indicating that the proximity effect of neighboring conductors induces some losses. The compact model of the inductor serves as a reasonable approximation for low frequency performance and gives some insight on the effects of the parasitic. The R_s does fluctuate with applied voltage, indicating that the proximity effect of neighboring conductors induces some losses. The C_s is very low since there is no coupling with an underlying metal layer, and the crosstalk between adjacent turns is not significant.

4 Conclusion

In this work a new variable inductor was designed, manufactured and tested. A liquid metal was used to vary the inductance. The fabricated tunable RF inductor demonstrates a wide tuning range of 400%. Inductance varied between 1.8 nH and 9.1 nH with a measured quality factor of 26 at 2 GHz, and the resonant frequency is 4 GHz. Variable inductance can be exploited in the design of mobile communication systems for new compatibility and improved electrical performance over a wide range and frequency. The inductor considered ambitious in terms of small size, power consumption and low cost. To implement this inductor in real applications, you would need some packaging or something to prevent liquid metal from moving.

5 Acknowledgments

The authors would like to thank the Deanship of Scientific Research at Umm Al-Qura University.

Funding: The authors would like to thank the Deanship of Scientific Research at Umm Al-Qura University for supporting this work by GRANT Code 23UQU4361156DSR02

6 Conflict of Interest

The authors declare no conflict of interest

7 References

1. Yao JJ. RF MEMS from a device perspective. *Journal of Micromechanics and Microengineering* 2000; 10: 9–38.
2. Yoon JB, Kim BK, Han CH et al. Surface micromachined solenoid on-Si and on glass inductors for RF applications. *IEEE Electron Device Letters* 1999; 20: 487–489.
3. Kral A, Behbahani F, Abidi AA RF-CMOS oscillators with switched tuning. *Proceedings of the IEEE in Custom Integrated Circuits Conference*; Santa Clara, CA; 1998: 555-558.
4. Young DH, Malba V, Ou JJ et al. A low-noise RF voltage-controlled oscillator using on-chip high Q three dimensional coil inductor and micromachined variable capacitor. *Proceedings of the Solid-State Sensor and Actuator Workshop*; Cleveland, OH, USA; 1998: 128-131.
5. J. J. Yao, "RF MEMS from a device perspective," *Journal of Micromechanics and Microengineering*, vol. 10, no. 4, pp. 9–38, Dec. 2000. <https://doi.org/10.1088/0960-1317/10/4/201>.
6. J.-B. Yoon, B.-K. Kim, C.-H. Han, E. Yoon, and C.-K. Kim, "Surface micromachined solenoid on-Si and on-glass inductors for RF applications," *IEEE Electron Device Letters*, vol. 20, no. 9, pp. 487–489, Sep. 1999. <https://doi.org/10.1109/55.784461>.
7. Yasser Mafinejad, Abbas Kouzani, Khalil Mafinezhad, «Review of low actuation voltage RF MEMS electrostatic switches based on metallic and carbon alloys», *Journal of Microelectronics, Electronic Components and Materials*, Vol. 43, No. 2 (2013), 85 – 96.
8. Alireza Ardehshiri, Gholamreza Karimi, Ramin Dehdasht-Heydari, «Optimization of shunt capacitive RF MEMS switch by using NSGA-II algorithm and utility algorithm» *Journal of Microelectronics, Electronic Components and Materials*, Vol. 49, No. 1(2019), 43 – 50,
9. Ahn CH, Allen MG. A planar micromachined spiral inductor for integrated magnetic micro actuator applications. *Journal of Micromechanics and Microengineering* 1999; 3: 37–44.
10. Fulcrand R, Bancaud A, Escriba C et al. On chip magnetic actuator for batch-mode dynamic manipulation of magnetic particles in compact lab-on-chip. *Sensors and Actuators B: Chemical* 2011; 160: 1520–1528.

11. Olivo J, Carrara S, De Micheli G. Micro-fabrication of high-thickness spiral inductors for the remote powering of implantable biosensors. *Microelectronic Engineering* 2014; 113: 130–135.
12. S. S. Bedair, J. S. Pulskamp, C. D. Meyer, M. Mirabelli, R. G. Polcawich, and B. Morgan, "High-performance micro machined inductors tunable by lead zirconate titanate actuators," *IEEE Electron Device Lett.*, vol. 33, no. 10, pp. 1483–1485, Oct. 2012. <https://doi.org/10.1109/LED.2012.2207700>.
13. M. B. Coskun, K. Thotahewa, Y.-S. Ying, M. Yuce, A. Neild, and T. Alan, "Nanoscale displacement sensing using micro fabricated variable inductance planar coils," *Appl. Phys. Lett.*, vol. 103, Oct. 2013, Art. no. 143501. <https://doi.org/10.1063/1.4823828>.
14. Araghchini M, Member S, Chen J et al. A technology overview of the power chip development program. *IEEE Transactions on Power Electronics* 2013; 28: 4182–4201
15. R. Wu, J. Chen, and X. Fang, "A novel on-chip transformer with patterned ground shield for high common-mode transient immunity isolated signal transfer," *IEEE Electron Device Lett.*, vol. 39, no. 11, pp. 1712–1715, Nov. 2018. <https://doi.org/10.1109/LED.2018.2871049>.
16. Y. Wang, Q. Zhang, L. Zhao, Y. Tang, A. Shkel, and E. S. Kim, "Vibration energy harvester with low resonant frequency based on flexible coil and liquid spring," *Appl. Phys. Lett.*, vol. 109, no. 20, 2016, Art. no. 203901. <https://doi.org/10.1063/1.4967498>.
17. J. Y. Park and J. U. Bu, "Packaging compatible micro transformers on a silicon substrate," *IEEE Trans. Adv. Packag.*, vol. 26, no. 2, pp. 160–164, May 2003. <https://doi.org/10.1109/tadvp.2003.817341>.
18. Yen-Chung Chiang and al, "A Study on the Variable Inductor Design by Switching the Main Paths and the Coupling Coils" *Electronics* 2021, 10, 1856. <https://doi.org/10.3390/electronics10151856>
19. Y. Yokoyama, T. Fukushige, S. Hata, K. Masu, and A. Shimokohbe, "On-chip variable inductor using micro electromechanical systems technology," *Jpn. J. Appl. Phys.*, vol. 42, no. 4B, p. 2190, 2003.
20. S. Zhou, X.-Q. Sun, and W. N. Carr, "A micro variable inductor chip using MEMS relays," in *Proc. Chicago Int. Conf. Solid State Sens. Actuators TRANSDUCERS*, vol. 2. Jun. 1997, pp. 1137–1140.
21. H. Sugawara, Y. Yoshihara, H. Ito, K. Okada, and K. Masu, "Wide range RF variable inductor on Si CMOS chip with MEMS actuator," in *Proc. 34th Eur. Microw. Conf.*, Oct. 2004, pp. 701–704.
22. H. Sugawara and al, "Variable RF inductor on Si CMOS chip," *Jpn. J. Appl. Phys.*, vol. 43, no. 4B, pp. 2293–2296, 2004.
23. J. M. Dell, K. Winchester, C. A. Musca, J. Antoszewski, and L. Faraone, "Variable MEMS based inductors fabricated from PECVD silicon nitride," in *Proc. Conf. Optoelectron. Microelectron. Mater. Devices*, Dec. 2002, pp. 567–570.
24. V. M. Lubecke, B. Barber, E. Chan, D. Lopez, M. E. Gross, and P. Gammel, "Self-assembling MEMS variable and fixed RF inductors," *IEEE Trans. Microw. Theory Techn.*, vol. 49, no. 11, pp. 2093–2098, Nov. 2001.
25. B. Assadsangabi, M. S. Mohamed Ali, and K. Takahata, "Ferfluidbased variable inductor," in *Proc. IEEE 25th MEMS Conf.*, Jan./Feb. 2012, pp. 1121–1124.
26. I. E. Gmati et al., "Fabrication and evaluation of an on-chip liquid micro-variable inductor," *J. Micro-mech. Microeng.*, vol. 21, no. 2, p. 025018, 2011.
27. Jyh-Chyurn Guo and Teng-Yang Tan, "A Broadband and Scalable Model for On-Chip Inductors Incorporating Substrate and Conductor Loss Effects." *IEEE TRANSACTIONS ON ELECTRON DEVICES*, VOL. 53, NO. 3, MARCH 2006.
28. Ahlberg, P. et al. Graphene as a Diffusion Barrier in Galinstain-Solid Metal Contacts. *IEEE Trans. Electron Devices* 1–5 (2014).
29. F. Khan, Y. Zhu, J. Lu, and J. Pal, "MEMS-based tunable meander inductor," *Electron. Letters* vol. 51, no. 20, pp. 1582–1583, Oct. 2015. <https://doi.org/10.1049/el.2015.2495>
30. A. Bhattacharya, D. Mandal, and T. K. Bhattacharyya, "A 1.3–2.4-GHz 3.1-mW VCO using electrothermo-mechanically tunable self-assembled MEMS inductor on HR substrate," *IEEE Trans. Microw. Theory Techn.*, vol. 63, no. 2, pp. 459–469, Feb. 2015. <https://doi.org/10.1109/TMTT.2014.2380357>
31. A. Shirane, H. Ito, N. Ishihara, and K. Masu, "Planar solenoid inductor in radio frequency micro-electro-mechanical systems technology for variable inductor with wide tunable range and high quality factor," *Jpn. J. Appl. Phys.*, vol. 51, no. 5S, p. 05EE02, May 2012. <https://doi.org/10.1143/JJAP.50.05EE01>
32. Tengxing W; Wei J; Ralu D; Daniel R; Leonidas E. O; Yujia P; Guoan W "Novel electrically tunable microwave solenoid inductor and compact phase shifter utilizing permalloy and PZT thin films," *IEEE Trans. Microw. Theory Techn.*, vol. 65, no. 10, pp. 3569–3577, Oct. 2017. doi <https://doi.org/10.1109/TMTT.2017.2731765>
33. H.Chen,X. Wang, Y. Gao, X. Shi, Z. Wang, N. Sun, M. Zaeimbashi, X. Liang, Y. He, C. Dong, Y. Wei, J.G. Jones, M.E. McConney, M.R. Page, B.M. Howe, G.J. Brown, N.-X. Sun "Integrated Tunable Magneto-electric RF Inductors". *IEEE Trans. Microw. Theory Tech.* 2020

- <https://doi.org/10.1109/TMTT.2019.2957472>
34. Yen-Chung Chiang, Juo-Chen Chen and Yu- Hsin Chang « A Study on the Variable Inductor Design by Switching the Main Paths and the Coupling Coils» *Electronics* 2021, 10, 1856.
- <https://doi.org/10.3390/electron- ics10151856>
35. Alexander M. Watson; Thomas F. Leary; Jonathan Itokazu; Aji G. Mattamana; Tony Quach; Aaron T. Ohta; Wayne A. Shiroma; Christopher E. Tabor “Tunable Microwave Inductor Using Liquid-Metal Microfluidics” 2021 IEEE Texas Symposium on Wireless and Microwave Circuits and Systems (WMCS), May 2021.
36. N. Lazarus and S. S. Bedair, “Bubble inductors: pneumatic tuning of a stretchable inductor,” *AIP Advances*, vol. 8, p. 056601, 2018.



Copyright © 2023 by the Authors.
This is an open access article distributed under the Creative Commons Attribution (CC BY) License (<https://creativecommons.org/licenses/by/4.0/>), which permits unrestricted use, distribution, and reproduction in any medium, provided the original work is properly cited.

Arrived: 21. 09. 2022
Accepted: 23. 02. 2023